Two-dimensional infrared spectroscopy of antiparallel beta-sheet secondary structure

Demirdoven, N; Cheatum, CM; Chung, HS; Khalil, M; Knoester, J; Tokmakoff, A; Demirdöven, Nurettin; Chung, Hoi Sung

Published in:
Journal of the American Chemical Society

DOI:
10.1021/ja049811j

Publication date:
2004

J|A|C|S
ARTICLES
Published on Web 06/02/2004

Two-Dimensional Infrared Spectroscopy of Antiparallel β-Sheet Secondary Structure

Nurettin Demirdöven,[†,§] Christopher M. Cheatum,[†,||] Hoi Sung Chung,[†] Munira Khalil,[†,⊥] Jasper Knoester,[‡] and Andrei Tokmakoff*[,†]

Contribution from the Department of Chemistry, Massachusetts Institute of Technology, Cambridge, Massachusetts 02139, and Materials Science Centre, University of Groningen, Nijenborgh 4, 9747 AG Groningen, The Netherlands

Received January 12, 2004; E-mail: tokmakof@mit.edu

Abstract: We investigate the sensitivity of femtosecond Fourier transform two-dimensional infrared spectroscopy to protein secondary structure with a study of antiparallel β-sheets. The results show that 2D IR spectroscopy is more sensitive to structural differences between proteins than traditional infrared spectroscopy, providing an observable that allows comparison to quantitative models of protein vibrational spectroscopy. 2D IR correlation spectra of the amide I region of poly-L-lysine, concanavalin A, ribonuclease A, and lysozyme show cross-peaks between the IR-active transitions that are characteristic of amide I couplings for polypeptides in antiparallel hydrogen-bonding registry. For poly-L-lysine, the 2D IR spectrum contains the eight-peak structure expected for two dominant vibrations of an extended, ordered antiparallel β-sheet. In the proteins with antiparallel β-sheets, interference effects between the diagonal and cross-peaks arising from the sheets, combined with diagonally elongated resonances from additional amide transitions, lead to a characteristic "Z"-shaped pattern for the amide I region in the 2D IR spectrum. We discuss in detail how the number of strands in the sheet, the local configurational disorder in the sheet, the delocalization of the vibrational excitation, and the angle between transition dipole moments affect the position, splitting, amplitude, and line shape of the cross-peaks and diagonal peaks.

Introduction

The infrared spectroscopy of protein amide transitions offers a powerful tool for the study of protein conformation and for probing the kinetics of protein conformational change. The amide vibrations of the protein reflect the couplings between the individual amide vibrations of the peptide units along the polypeptide backbone. The strength of the couplings and the energies of the local peptide vibrations are in turn dictated by the protein conformation and hydrogen bonding to the peptide units. These couplings give rise to delocalized (or excitonic) vibrational states that involve many amide vibrations, leading to infrared transition frequencies that are characteristic of different secondary structures.[1−4] Extensive qualitative evidence correlates characteristic amide I absorption frequencies with the presence of α-helices (∼1650 cm^{-1}), β-sheets ($\leq$1640 cm^{-1} and $\geq$1680 cm^{-1}), and random coils (∼1640−1650 cm^{-1}).[4−6] Infrared spectroscopy is thus an appealing probe because it is intrinsic to all proteins and is sensitive to conformation and mesoscopic structure. Moreover, as a method with intrinsic time resolution in the picosecond range, infrared methods can be applied to study the fast kinetics of protein conformational changes accompanying protein folding.[7]

Even with these potential advantages, such correlations are difficult to apply in the case of proteins with congested amide I spectra,[5] and traditional protein infrared spectroscopy remains a largely qualitative method. Its limitations as a quantitative tool for revealing structural details about protein conformation have two primary origins. First, infrared (IR) spectra of proteins are generally broad and featureless due to overlapping contributions from many vibrations, thereby hiding any structural selectivity of the resonances. This is partially because the amide vibrations of proteins are susceptible to local configurational variation in the protein that results in inhomogeneous broadening of the absorption line shapes. Second, the quantitative relationships linking the frequency and amplitude of IR resonances to the underlying protein structure are not entirely understood. Developing models for the vibrational spectroscopy of proteins requires an understanding of amide vibrational couplings and of peptide electronic structure including intermolecular interac-

[†] Massachusetts Institute of Technology.
[‡] University of Groningen.
[§] Present address: Technology and Policy Program, Massachusetts Institute of Technology.
[||] Present address: Department of Chemistry, University of Iowa.
[⊥] Present address: Department of Chemistry, University of California, Berkeley.

(1) Krimm, S.; Bandekar, J. *Adv. Protein Chem.* **1986**, *38*, 181.
(2) Torii, H.; Tasumi, M. *J. Chem. Phys.* **1992**, *95*, 3379. Torii, H.; Tasumi, M. *J. Chem. Phys.* **1992**, *97*, 92.
(3) Choi, J. H.; Ham, S.; Cho, M. *J. Chem. Phys.* **2002**, *117*, 6821.
(4) Barth, A.; Zscherp, C. *Q. Rev. Biophys.* **2002**, *35*, 369.
(5) Surewicz, W. K.; Mantsch, H.; Chapman, D. *Biochemistry* **1993**, *32*, 389.
(6) Haris, P. I.; Chapman, D. *Trends Biochem. Sci.* **1992**, *17*, 328. Susi, H.; Byler, D. M. *Methods Enzymol.* **1986**, *130*, 290.
(7) Dyer, R. B.; Gai, F.; Woodruff, W. H.; Gilmanshin, R.; Callender, R. H. *Acc. Chem. Res.* **1998**, *31*, 709. Bredenbeck, J.; Helbing, J.; Behrendt, R.; Renner, C.; Moroder, L.; Wachtveitl, J.; Hamm, P. *J. Phys. Chem. B* **2003**, *107*, 8654.

tions that influence it, such as hydrogen bonding. For testing such models, traditional IR spectroscopy is not a sensitive probe. Some improvement in selectivity is possible with vibrational circular dichroism, which draws on the noncentrosymmetric nature of protein structure.[8]

A number of the difficulties of studying proteins with traditional IR spectroscopy can be overcome with femtosecond two-dimensional infrared (2D IR) spectroscopy. In a manner analogous to Fourier transform 2D NMR spectra, 2D IR spectra spread the vibrational resonances over two frequency dimensions, revealing couplings between vibrations through the formation of cross-peaks in the spectrum.[9−11] For small molecules, these 2D IR spectra have been used to obtain information on three-dimensional structure and conformational variation by modeling the coupling between vibrational coordinates of the molecule.[11−14] 2D IR spectra also help overcome inhomogeneous broadening and even characterize the underlying structural variation.[13,15,16] Using these characteristics, 2D IR spectra of peptides have been described in terms of delocalized vibrational states arising from multiple coupled oscillators.[17,18]

To investigate the sensitivity of 2D IR spectroscopy to protein secondary structure and the delocalization of amide vibrations, we report on the 2D IR signatures of antiparallel (AP) β-sheets in the amide I spectral range. Experiments were performed on a model polypeptide, poly-L-lysine, in an AP β-sheet conformation and three globular proteins with AP β-sheet domains. AP β-sheets were chosen because they are an abundant secondary structure in globular proteins and constitute a biologically important class of mesoscopic structure involved in protein aggregation and fibril formation.[19] Additionally, IR spectra indicate that AP β-sheets, with two amide I transitions, one strong between 1610 and 1640 cm^{-1} and another weak transition between 1680 and 1700 cm^{-1}, should be more clearly resolved in the IR spectroscopy than other secondary structures.[1,20] Our 2D IR experiments reveal the formation of cross-peaks between the two IR-active transitions of the AP β-sheet. The cross-peaks are clear and well-resolved for large extended β-sheets and become stretched out or elongated for smaller sheets. In proteins, interference effects between diagonal and cross-peaks, combined with contributions from disordered regions and other secondary structures, lead to a "Z"-shaped contour profile in the 2D IR amide I correlation spectrum that is a characteristic indicator of the presence of AP β-sheet secondary structure.

In the following, we outline the origin of the β-sheet 2D IR spectra in terms of the vibrational couplings of polypeptides in antiparallel hydrogen-bonding registry and the conformational variation in such structures. This discussion draws on comparisons between our experimental results and the predictions of a recent theory for the 2D IR spectroscopy of β-sheets.[21] Specifically, we discuss below how the position, splitting, amplitude, and line shape of the cross-peak and diagonal peaks can be related to (a) the size of the sheet, (b) the strength of vibrational couplings within the sheet, (c) the extent of delocalization of the vibrational excitation, (d) conformational variation of the β-sheet, and (e) the projection angle between the transition dipole moments for β-sheet vibrational transitions. The results lead us to conclude that 2D IR spectroscopy is a sensitive measure of protein AP β-sheet structure. We also suggest that, although the structural information obtained is not atomistic in nature, by probing delocalized vibrations 2D IR spectroscopy is an effective measure of conformation, and its sensitivity to disorder in short-range interactions makes it a probe of heterogeneity. It therefore has the potential to become an important structural probe of protein kinetics and dynamics in solution with a picosecond time-window.

Methods and Materials

Materials. Poly-L-lysine HCl was purchased from Sigma Aldrich and used without further purification. The molecular weight (MW) was approximately 70 000−150 000 Da. Poly-L-lysine samples were dissolved in D_2O and allowed to undergo hydrogen−deuterium exchange for 2 h. The pD of the sample was adjusted to 12.2 by adding small amounts of 1 M NaOD and/or 1 M DCl. The sample concentration was 22 mg/mL (2.0% w/w). Concanavalin A (Con A, source: jack bean, 237 residues, MW 26 583, Protein Data Bank ID 1NLS), ribonuclease A (RNase A, source: bovine pancreas, 124 residues, 13 674, PDB ID 1FS3), lysozyme (source: chicken egg white, 129 residues, MW 14 296, PDB ID 132L), and myoglobin (source: horse skeletal muscle, 153 residues, MW 16 935, PDB ID 1WLA) were also purchased from Sigma Aldrich. Con A, RNase A, and myoglobin were dissolved in phophate/D_2O buffer at pD 7.6, and lysozyme at pD 5.5. Protein concentrations were approximately ~15 mg/mL. PD's of the samples are calculated according to pD = 0.34668 + 1.0369·pH. All protein samples were allowed to undergo hydrogen−deuterium exchange for 2 h.

FTIR Measurements. Samples were held in a home-built, temperature-controlled cell with 1-mm thick calcium fluoride windows and a 50-μm path length. The optical densities of the samples were ≤0.2. The FTIR spectra were obtained using a Mattson Infinity Gold FTIR spectrometer with a spectral resolution of 2 cm^{-1} and a D_2O solvent background. The FTIR spectrum of PLys was recorded at 46 °C. All of the other protein FTIR spectra were taken at ambient temperature (20 °C).

2D IR Spectroscopy. The details of the 2D IR spectrometer, the principles used to obtain 2D IR correlation spectra, and the structural and dynamical information content of these spectra have been described in detail elsewhere.[11,22] Here, we summarize those features of the spectroscopy relevant to the discussion of the data below.

In Fourier transform 2D IR spectroscopy, three femtosecond mid-IR pulses resonant with the amide I transitions are crossed in the sample. The short pulses have a sufficiently broad spectral bandwidth such that they are resonant both with the fundamental ($v = 0 \rightarrow 1$) amide I transitions, as well as with the transitions between the anharmonically shifted $v = 1 \rightarrow 2$ transitions. These pulses sequentially drive absorption

(8) Keiderling, T. A. *Curr. Opin. Chem. Biol.* **2002**, *6*, 682.
(9) Zanni, M. T.; Gnanakaran, S.; Stenger, J.; Hochstrasser, R. M. *J. Phys. Chem. B* **2001**, *105*, 6520.
(10) Woutersen, S.; Hamm, P. *J. Phys.: Condens. Matter* **2002**, *14*, R1035.
(11) Khalil, M.; Demirdöven, N.; Tokmakoff, A. *J. Phys. Chem. A* **2003**, *107*, 5258.
(12) Woutersen, S.; Hamm, P. *J. Chem. Phys.* **2001**, *114*, 2727. Zanni, M. T.; Stenger, J.; Asplund, M. C.; Hochstrasser, R. M. *Biophys. J.* **2001**, *80*, 38. Zanni, M.; Ge, N.-H.; Kim, Y. S.; Hochstrasser, R. M. *Proc. Natl. Acad. Sci. U.S.A.* **2001**, *98*, 11265.
(13) Woutersen, S.; Mu, Y.; Stock, G.; Hamm, P. *Proc. Natl. Acad. Sci. U.S.A.* **2001**, *98*, 11254.
(14) Golonzka, O.; Khalil, M.; Demirdöven, N.; Tokmakoff, A. *J. Chem. Phys.* **2001**, *115*, 10814.
(15) Zanni, M. T.; Gnanakaran, S.; Stenger, J.; Hochstrasser, R. M. *J. Phys. Chem. B* **2001**, *105*, 6520. Woutersen, S.; Pfister, R.; Hamm, P.; Mu, Y. G.; Kosov, D. S.; Stock, G. *J. Chem. Phys.* **2002**, *117*, 6833.
(16) Demirdöven, N.; Khalil, M.; Tokmakoff, A. *Phys. Rev. Lett.* **2002**, *89*, 237401.
(17) Hamm, P.; Lim, M.; Hochstrasser, R. M. *J. Phys. Chem. B* **1998**, *102*, 6123.
(18) Woutersen, S.; Hamm, P. *J. Chem. Phys.* **2001**, *115*, 7737.
(19) Searle, M. S. *J. Chem. Soc., Perkin Trans. 2* **2001**, *7*, 1011.
(20) Miyazawa, T. *J. Chem. Phys.* **1960**, *32*, 1647.
(21) Cheatum, C. M.; Tokmakoff, A.; Knoester, J. *J. Chem. Phys.* **2004**, *120*, 8201.
(22) Khalil, M.; Demirdöven, N.; Tokmakoff, A. *Phys. Rev. Lett.* **2003**, *90*, 47401.

and stimulated emission processes between the $v = 0$, 1, and 2 vibrational states. Following each pulse, the system evolves freely during three sequential time intervals, τ_i. The third field stimulates the radiation of a background-free nonlinear signal field. We characterize the coherent vibrational excitations sampled during the two time periods following the initial excitation and following the final pulse during the radiation of the signal (τ_1 and τ_3), and we represent these as a 2D Fourier transform spectrum in ω_1 and ω_3.

Our experiments were performed with 90 fs mid-IR pulses ($\lambda = 6$ μm) with a fwhm bandwidth of 160 cm^{-1}.[11,23] Three independently timed pulses were focused into the sample with incident wave vectors $\mathbf{k}_a$, $\mathbf{k}_b$, and $\mathbf{k}_c$ to generate the signal field along the phase-matched direction $\mathbf{k}_s = -\mathbf{k}_a+\mathbf{k}_b+\mathbf{k}_c$. In practice, the time-profile of the radiated signal field is characterized by heterodyne detection. After the sample, the signal field was temporally and spatially overlapped with a fourth local oscillator pulse, focused into a 190-mm monochromator, and dispersed by a 40-lines/mm grating onto a 64-channel mercury−cadmium−telluride (MCT) array detector at the focal plane. In this detection scheme, the monochromator acts to effectively Fourier transform the heterodyned signal field with respect to τ_3, leading to a spectral resolution of ~4 cm^{-1} in the ω_3 dimension. A series of such interferograms are collected by sweeping τ_1 to a delay of ~3 ps with 3 fs steps. Timing delays were controlled with Aerotech ANT-50L stages, which have a resolution of 10 nm (0.067 fs) and were found to have an accuracy of 300 nm (2 fs) and a repeatability of 50 nm (0.33 fs). The resulting (τ_1,ω_3) 2D matrix is Fourier transformed along τ_1 to obtain the corresponding 2D spectrum in (ω_1,ω_3). The final 2D IR correlation spectrum has absorptive line shapes as a result of summing two independent, complementary spectra (rephasing and nonrephasing).[22] These differ in the phase acquired by coherences during τ_1: $\exp(i\Omega\tau_1)$ for rephasing and $\exp(-i\Omega\tau_1)$ for nonrephasing. The phasing of the 2D correlation spectrum follows previously described procedures to match a dispersed pump−probe measurement.[24] For the experiments shown here, $\tau_2 = 0$. The entire experimental setup is purged with dry air to minimize the effects of atmospheric water absorption. The sample concentrations were adjusted to correspond to a peak optical density of ≤0.2. The intensity of each beam is adjusted by wire-grid polarizers and half-wave plates to ensure equal excitation power at different polarization conditions. Protein 2D IR spectra were taken in the crossed polarization geometry (ZZYY). Polarization-dependent anisotropy measurements were made by comparison of matched measurements in parallel (ZZZZ) and crossed geometries.

Results and Discussion

A. Model for β-Sheet 2D IR Spectroscopy. Vibrational States of β-Sheets. The conformational sensitivity of protein infrared bands was first shown in the pioneering works of Elliot and Ambrose, who established empirical correlations between folded and extended forms of synthetic polypeptides and their vibrational transitions.[25] These studies were followed by the primary theoretical analyses of amide I vibrations in relation to conformation of proteins by Miyazawa[20,26] and Krimm,[27] who described how absorption patterns in amide I spectra can be explained by the symmetry of the structure and short-range couplings between the amide I vibrations. The relatively strong couplings between the many amide I vibrations of the polypeptide backbone interact, leading to collective vibrations (exciton states) characterized by the symmetry of the secondary structure.[20] These observations, which have been reviewed in detail,[1,4] form the basis for our vibrational exciton model of the traditional IR and 2D IR spectroscopy of amide I transitions arising from idealized antiparallel (AP) β-sheets.[21] (The amide I vibration for a peptide unit is roughly 80% CO stretching vibration, with the remaining motion in out-of-phase CN stretching and CCN deformation.[1]) Building on the approaches of Miyazawa[20,26] and Chirgadze,[28] AP β-sheets and β-hairpins of a given size and geometry were constructed with a lattice of unit cells containing four peptide groups, which are replicated parallel and perpendicular to the polypeptide strand. Within the unit cell, pictured in Figure 1, the four peptide units were positioned such that the torsion angles along the backbone are (ϕ,ψ) = (−160°,-118°), and the interstrand separation between O and N along linear C═O···H−N hydrogen bonds is 3.04 Å. The vibrational eigenstates for these sheets were calculated as a set of coupled anharmonic oscillators. The amide I vibrational potential at the peptide units was represented with a set of degenerate anharmonic oscillators with a fundamental frequency $\omega_{10} = 1675$ cm^{-1} and a site anharmonicity of $A = \omega_{10} - \omega_{21} = 16$ cm^{-1}. Couplings between these oscillators were calculated from transition dipole interactions using Krimm's parametrization for the magnitude, position, and orientation of the dipoles.[1] The strongest interactions are dictated by the proximity of the amide dipoles and the general alignment of the transition dipoles perpendicular to the direction of the strands.

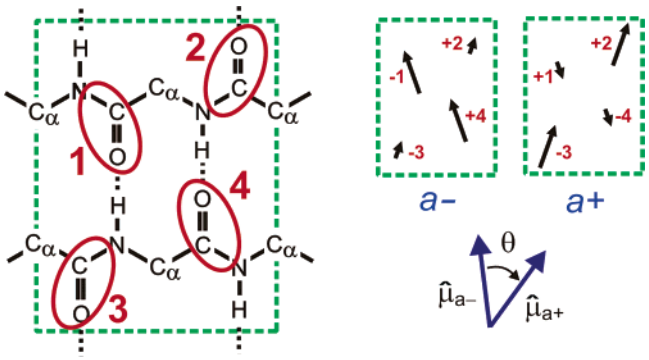

Figure 1. (Left) A top-down view of the unit cell (6.88 Å × 10.08 Å) for an idealized pleated antiparallel β-sheet, where C_α bonds to the side chains are oriented out of the plane. The four local amide I transitions (primarily CO stretch with CN stretching and CCN bending) are labeled. In the transition dipole coupling model, the significant couplings (L_{ij}) between amide I vibrations are: $L_{14} = 19$ cm^{-1}, $L_{24} = L_{13} = -7.4$ cm^{-1}, $L_{23} = 1.5$ cm^{-1}, $L_{34} = L_{12} = 1$ cm^{-1}.[21] (Right) The amplitude and phase of the local amide I vibrations contributing to the dominant infrared active $a-$ and $a+$ eigenstates are shown, together with the orientation of the unit vectors along their transition dipole moments $\boldsymbol{\mu}$.

Characterization of the vibrational eigenstates (or exciton states) for this model allowed certain predictions to be made regarding the amide I IR spectroscopy of AP β-sheet structures.[21] For the unit cell, there are four vibrational eigenstates which involve the permutations in phases for the four vibrational coordinates. These are labeled $a+$, $a-$, $s+$, and $s-$, where s and a refer to symmetric (in-phase) and antisymmetric (out-of-phase) stretching of the 1−4 and 2−3 pairs, and for the a states, $+$ and $-$ refer to in-phase and out-of-phase evolution, respectively, of oscillators 1 and 2. The infrared oscillator strength is carried primarily by the strong $a-$ transition and the weaker $a+$ transition. For larger β-sheets, the IR spectrum is still

(23) Demirdöven, N.; Khalil, M.; Golonzka, O.; Tokmakoff, A. *Opt. Lett.* **2002**, *27*, 433.
(24) Hybl, J. D.; Ferro, A. A.; Jonas, D. M. *J. Chem. Phys.* **2001**, *115*, 6606.
(25) Elliott, A.; Ambrose, E. J. *Nature* **1950**, *165*, 921. Ambrose, E. J.; Elliot, A. *Proc. R. Soc. London, Ser. A* **1951**, *205*, 47.
(26) Miyazawa, T.; Blout, E. R. *J. Am. Chem. Soc.* **1961**, *83*, 712.
(27) Krimm, S.; Abe, Y. *Proc. Natl. Acad. Sci. U.S.A.* **1972**, *69*, 2788.
(28) Chirgadze, Y. N.; Nevskaya, N. A. *Biopolymers* **1976**, *15*, 607.

dominated by transitions to $a+$ and $a-$ vibrational states. These states represent the same phase relationship between amide oscillators as the unit cell, involving the asymmetric vibration of the nearest-neighbor interstrand dimers such as the 1−4 pair, and either in-phase (+) or out-of-phase (−) oscillation between the nearest amide I oscillators along the strands. In the limit of an infinite sheet, the $a+$ and $a-$ modes correspond to the $\nu(0,\pi)$ and $\nu(\pi,0)$ modes of Miyazawa.[20] The fundamental transition energy to the $a+$ state is roughly $\omega_{a+} \approx 1680$ cm^{-1}, and its frequency and amplitude are insensitive to the size of the sheet. The $a-$ mode is sensitive to the dimensions of the sheet, red-shifting from $\omega_{a-} = 1655$ cm^{-1} to an asymptotic value of 1635 cm^{-1} as the sheet grows perpendicular to the strands. These observations suggest that spectral broadening of the $a-$ transition will be affected by conformational variation within AP β-sheet structures to a far greater extent than the $a+$ transition. Calculations show that the $a-$ transition dipole moment $\boldsymbol{\mu}_{a-}$ is oriented roughly perpendicular to the strand direction. The angle between it and the transition moment for the $a+$ mode $\boldsymbol{\mu}_{a+}$, which also lies in the plane of the sheet, varies from $\theta = 41°$ for the unit cell to $\theta = 65-70°$ for extended sheets.

The size-dependent trends in the energies of the β-sheet vibrational states can be rationalized in terms of the geometry of the amide I transition dipoles in the AP β-sheet and the strongest short-range couplings. For a unit cell, the energy shift of the $a-$ and $a+$ states can be expressed in terms of the various couplings L_{ij} between amide I vibrations i and j: $E_{a\pm} - \hbar\omega_{10} = -(L_{14} + L_{23})/2 \pm \sqrt{((L_{14}-L_{23})/2)^2+(L_{24}-L_{12})^2}$. The $a-$ frequency shift is dominated by the strongest couplings, the roughly 20 cm^{-1} interstrand interaction between nearest amide I carbonyls, L_{14}, and somewhat weaker interstrand interactions ($L_{24} \approx -7$ cm^{-1}). The addition of each additional strand to a sheet also adds further strong interstrand amide I couplings, leading to further delocalization of the amide I excitation and concurrent red-shifts of the $a-$ band. The other couplings in our model are relatively weak. The intrastrand coupling $L_{12} = L_{34} \approx 1$ cm^{-1} lies within the range of values (−7 to +9 cm^{-1}) obtained from ab initio calculations on dipeptides and for the range of (ϕ,ψ) associated with AP β-sheets.[10,29,30] Within the transition dipole coupling model, the magnitudes of all interactions between unit cells along the polypeptide strands are ≤4 cm^{-1}.

Features of 2D IR Spectra. In principle, 2D IR spectroscopy can be used to reveal the split $a+$ and $a-$ transitions, even when the traditional IR spectrum is congested. Figure 2 shows calculated linear-IR and 2D IR correlation spectra for an idealized extended β-sheet obtained from a 3 × 3 array of AP β-sheet unit cells, using the methods described in ref 21. For calculations with periodic boundary conditions, which include all of the couplings within the 3 × 3 sheet but otherwise treat the sheet as infinite, the IR spectrum shows two transitions, the dominant $a-$ line at $\omega_{a-} = 1633$ cm^{-1} and the $a+$ line at $\omega_{a+} = 1681$ cm^{-1}. The 2D IR correlation spectrum reveals these resonances through four peaks, two diagonal peaks and two cross-peaks, each of which is split into an oppositely signed doublet displaced along the ω_3 dimension.

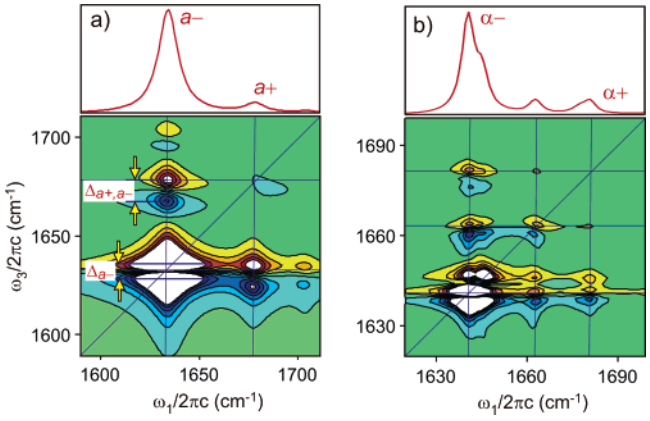

Figure 2. Calculated infrared (top) and 2D IR correlation spectra (bottom) for an idealized extended β-sheet composed of a 3 × 3 lattice of the unit cells in Figure 1. Calculations are for (a) periodic boundary conditions and (b) open boundary conditions. The 2D IR calculations assume a crossed polarization (ZZYY) condition. We have used Lorentzian line shapes with a width of (a) $\gamma = 4$ cm^{-1} and (b) $\gamma = 2.5$ cm^{-1}. Positive features are shown in red, and negative features are shown in blue. Equally spaced contours are plotted between −10% and 10% of the $a-$ diagonal peak maximum.

The first dimension ω_1 represents the frequency of the initially excited fundamental transition, and the second dimension ω_3 represents the transition from which the signal was finally radiated following interactions with the second and third pulses. The positive peaks arise from signals radiated from the fundamental ($v = 1$) $a+$ and $a-$ transitions. The negative peaks are radiated from the $v = 2 \rightarrow 1$ transitions, for which transitions from the $v = 2$ overtones (two quanta of $a+$ or $a-$) contribute to the diagonal peak and transitions from $v = 2$ combination bands (bi-exciton with one quantum in both $a+$ and $a-$) contribute to the cross-peak.[11,31] While underlying couplings cannot be deduced from traditional IR spectra of fundamental transitions, the formation of cross-peaks in the 2D IR spectrum is a direct indication of the vibrational couplings between the local peptide vibrations leading to the $a+$ and $a-$ vibrational transitions. The overall magnitude of the amide I couplings is reflected both in the frequency splitting between the $a-$ and $a+$ states $\omega_{a+,a-} = (\omega_{a+} - \omega_{a-})$ and in the splitting of the cross-peak in the ω_3 dimension $\Delta_{a+,a-}$. The anharmonic splitting $\Delta_{a+,a-}$ represents the energy shift of the doubly vibrationally excited $a+/a-$ combination band relative to the sum of the $a-$ and $a+$ fundamental energies and is thus a direct measure of the coupling between the peptide units.[11,14,31] The value of the anharmonic splitting of the diagonal and cross-peaks also reflects the number of oscillators over which the excitation is delocalized, N. For a set of degenerate amide I oscillators with a site anharmonicity A, the splitting between the negative and positive lobes of the diagonal peak is expected to scale as A/N when this quantity is greater than the line width γ.[21] In the 2D IR spectrum of a massively delocalized excitation, such as that calculated in Figure 2a, the oppositely signed peaks of the doublet are closer to coincident and interfere leaving a node in the spectrum for those values of ω_3 equal to the fundamental transitions. In this limit, the splitting of the diagonal peak is approximately equal to the line width γ.

(29) Torii, H.; Tasumi, M. *J. Raman Spectrosc.* **1998**, *29*, 81.
(30) Ham, S.; Cho, M. *J. Chem. Phys.* **2003**, *118*, 6915.
(31) Golonzka, O.; Khalil, M.; Demirdöven, N.; Tokmakoff, A. *Phys. Rev. Lett.* **2001**, *86*, 2154.

The cross-peak amplitude has considerably higher intensity than the $a+$ diagonal peak and clearly reveals the existence of the weak $a+$ transition. The amplitudes of the peaks in the 2D IR spectrum scale nonlinearly in the transition dipole moment.[32] For a spectrum of two coupled vibrations b and c, the amplitude scales roughly as $|\mu_b|^4$ and $|\mu_c|^4$ for diagonal peaks, and $|\mu_b|^2|\mu_c|^2$ for cross-peaks. Therefore, cross-peaks between strong and weak transitions can be used to reveal those transitions hidden in the linear spectrum. This is further illustrated in Figure 2a, where cross-peaks are observed between the $a-$ transition and the very weak, out-of-plane $s+$ transition at $\omega_{s+} = 1705$ cm^{-1}. The amplitude of the cross-peaks also depends on the projection of the input field polarizations onto the transition dipole moments that lead to the peak.[11,33] By measuring the variation of the cross-peak amplitude for different polarizations of the input fields, the relative orientation of the transition moments can be determined.[11−14]

Figure 2 also shows the linear-IR and 2D IR spectra calculated for a finite 3 × 3 sheet using open boundary conditions that include the effect of mixed-symmetry eigenstates that result from the edges of the sheet. The same two dominant split peaks are observed, now at 1641 and 1681 cm^{-1}, although each now shows shoulders from other transitions. The dominant transitions still retain the phase relationship between oscillators observed in the unit cell. The additional transitions still involve asymmetric vibrations of the strongly coupled interstrand dimers, but may have phase relationships between the dimers that vary from the ideal $a-$ and $a+$ states of an infinite ordered sheet. To distinguish the strong peaks in the spectrum for finite or disordered sheets that may result from overlapping transitions of slightly varying symmetry from the $a-$ and $a+$ designation used for the unit cell, we label them α− and α+. The calculations also show that edge effects in the finite system lead to additional transitions in the 1660−1665 cm^{-1} region.[21,28,34] These peaks do not correspond to any of the transitions found in the unit cell, but result from states of mixed symmetry character. They also lead to additional cross-peaks with the α− and α+ resonances.

It should be noted that, in addition to the magnitude and orientation of the transition dipole moments, the amplitudes of the peaks in the 2D IR spectrum are also influenced by interference effects between resonances, particularly when the peak splittings and line widths are comparable. In Figure 2, the cross-peak observed for $\omega_1 > \omega_3$ has a higher amplitude than that for $\omega_1 < \omega_3$. This is a result of the constructive interference along the ω_1 axis between positive and negative features of the diagonal and cross-peaks doublets. More generally, in congested spectra such as those with additional transitions involving states of mixed symmetry at ∼1660 cm^{-1}, these same constructive interference effects will lead to the observation of ridges along ω_1, whereas such overlap will destructively interfere along ω_3.

B. 2D IR Spectroscopy of Poly-L-Lysine. To test the predictions of the vibrational exciton model for extended β-sheets, we first measured the 2D IR spectra of poly-L-lysine (PLys). At pH > 10 and temperature > 30 °C, PLys shows IR and UV circular dichroism spectra consistent with those of an extended AP β-sheet conformation.[35,36] Similar to the theoretical

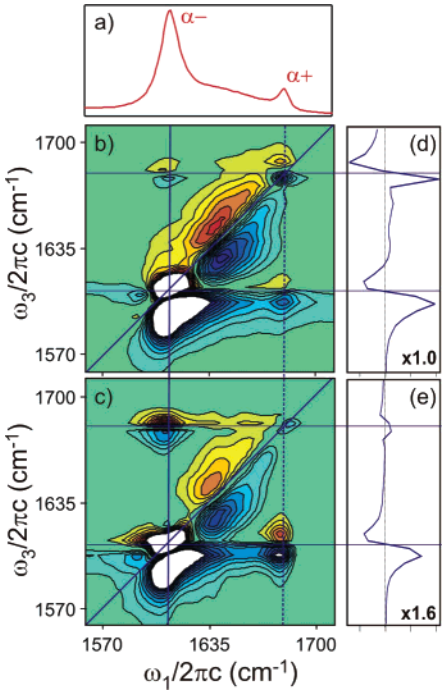

Figure 3. (a) FTIR spectrum of poly-L-lysine at high pD. 2D IR correlation spectra of PLys for the (b) parallel (ZZZZ) and (c) crossed (ZZYY) polarization geometries. Nineteen equally spaced contours are plotted between −20% and 20% of the peak maximum. Slices at $\omega_1 = 1680$ cm^{-1} (dashed line) are plotted for (d) ZZZZ and (e) ZZYY. The projection angle between $\boldsymbol{\mu}_{\alpha+}$ and $\boldsymbol{\mu}_{\alpha-}$ is determined from the observed cross-peak amplitude ratio in these slices.

predictions for an extended sheet, the FTIR spectrum of PLys (Figure 3a) shows two distinct amide I resonances with narrow line widths ($\gamma = 8$ cm^{-1} HWHM), one strong, lower frequency transition at 1611 cm^{-1} and one weak, higher frequency transition at 1680 cm^{-1}. The position and amplitude of these resonances are consistent with the predictions for the α− and α+ resonances of an infinite β-sheet although with somewhat stronger couplings and lower site energies than our model. The extreme red-shift of the α− band is consistent with other studies of β-sheet aggregates.[36,37] Additionally, the sharp α− and α+ resonances sit on top of a broad low-amplitude feature that peaks at 1635 cm^{-1}, which has been attributed to a range of short length chains.[36]

The 2D IR correlation spectrum of PLys, shown in Figure 3b and 3c for parallel and crossed polarization geometries, reveals features that are expected for an ordered extended β-sheet. The features in the spectrum can be described in terms of the position, amplitudes, and line shapes of the resonances. Clear cross-peaks are seen between the α− and α+ resonances at $(\omega_1,\omega_3) = (1611,1680)$ and $(1680,1611)$ cm^{-1}. Much like the model calculation, an eight-peak structure is observed, as would be expected when vibrational couplings lead to two split

(32) Khalil, M.; Tokmakoff, A. *Chem. Phys.* **2001**, *266*, 213.
(33) Hochstrasser, R. M. *Chem. Phys.* **2001**, *266*, 273. Golonzka, O.; Tokmakoff, A. *J. Chem. Phys.* **2001**, *115*, 297.
(34) Kubelka, J.; Keiderling, T. A. *J. Am. Chem. Soc.* **2001**, *123*, 6142.
(35) Susi, H.; Timasheff, S. N.; Stevens, L. *J. Biol. Chem.* **1967**, *242*, 5460. Chirgadze, N. Y.; Shestopa, B. V.; Venyamin, S. Y. *Biopolymers* **1973**, *12*, 1337.
(36) Jackson, M.; Haris, P. I.; Chapman, D. *Biochim. Biophys. Acta* **1989**, *998*, 75.
(37) Byler, D. M.; Susi, H. *Biopolymers* **1986**, *25*, 469. Surewicz, W. K.; Mantsch, H. *Biochim. Biophys. Acta* **1988**, *952*, 115. Kalnin, N. N.; Baikalov, I. A.; Venyaminov, S. Y. *Biopolymers* **1990**, *30*, 1273. Venyaminov, S. Y.; Kalnin, N. N. *Biopolymers* **1990**, *30*, 1259. van Stokkum, I. H.; Linsdell, H.; Hadden, J. M.; Haris, P. I.; Chapman, D.; Bloemendal, M. *Biochemistry* **1995**, *34*, 10508. Silva, R. A. G. D.; Barber-Armstrong, W.; Decatur, S. M. *J. Am. Chem. Soc.* **2003**, *125*, 13674.

vibrational transitions. The formation of these cross-peaks confirms the assignment of the α− and α+ transitions and is a clear marker of AP β-sheet structure. Even in congested spectra where peaks are predominantly clustered along the diagonal axis, these off-diagonal features should be resolved.

The amplitude of the cross-peak has considerably higher intensity than the diagonal peak of transition α+ and clearly reveals the existence of the weak transition α+. This arises from the scaling of the cross-peak amplitude in the square of the transition dipole moment of the two transitions. Although this scaling relationship does significantly help in revealing weak features, we do not see any evidence of cross-peaks to the very weak *s*+ transition predicted at $\omega > 1700$ cm^{-1} in Figure 2a.

A comparison of the cross-peak amplitudes in the parallel and crossed polarization configurations can be used to determine the projection angle between the α− and α+ transition dipole moments of PLys.[11,14] Also shown in Figure 3 are slices for $\omega_1 = 1680$ cm^{-1} from the polarization anisotropy measurement. From an analysis of both cross-peaks in parallel and crossed polarization configurations, we obtain a cross-peak amplitude ratio of 0.82 ± 0.15. This ratio correlates with a projection angle of $\theta = 65° \pm 10°$, which agrees well with our predictions for large finite sheets. A value of ∼70° is expected for extended systems with greater than eight strands.[21] The value of θ and the error bars can also be confirmed by separately analyzing the peak amplitude ratios in the constituent rephasing and nonrephasing spectra, as described in the Supporting Information.

The large splitting between the fundamental resonances $\omega_{\alpha+,\alpha-}$ is consistent with the expectation of strong interstrand amide I couplings in an ordered AP β-sheet structure. At the same time, the splitting of the diagonal and cross-peaks is on the order of the vibrational line width ($\Delta_{\alpha-}$; $\Delta_{\alpha+,\alpha-} < 8$ cm^{-1}) and less than the amide I anharmonicity, leading to a node on resonance along ω_3. These observations suggest a considerable delocalization of the vibrational transition in the direction perpendicular to the strands. Because the diagonal peak splitting $\Delta_{\alpha\pm}$ has reached the limiting value of γ, this delocalization is probably spread over several strands. Within our idealized model, the measurement of $\theta = 65°$ is also consistent with delocalization of greater than eight strands. This suggests that, for polypeptides and aggregated proteins that self-assemble into AP β-sheet structures, the amide I vibrational excitations can be delocalized over nanometer distances. This is a result of strong interstrand couplings in a sheet with an ordered and relatively planar geometry and only weak energetic disorder to the peptide vibration due to a very regular hydrogen-bonding geometry between strands.

An elongated feature is observed on the diagonal axis ($\omega_1 = \omega_3$) peaking at 1640 cm^{-1}, which corresponds to the broad background feature observed in the FTIR spectrum. Its 2D IR line shape is a diagonally elongated ellipsoid, indicating an inhomogeneous line shape.[11,38] This arises both from disordered or loop regions of the polypeptide strands and from the additional β-sheet transitions shown in Figure 2b that are expected for finite sheets. Although narrow, the line shapes of the diagonal α+ and α− resonances are also slightly elongated along the diagonal axis, showing that some inhomogeneity remains in the dominant α+ and α− β-sheet transitions. The cross-peaks, on the other hand, are broadened parallel to the ω_1 axis. This can be attributed to three effects: inhomogeneity of the α− transition, a cross-peak splitting $\Delta_{\alpha+,\alpha-} < \gamma$, and constructive interferences in the wings of the line shapes between the positive and negative lobes of the diagonal and cross-peaks.

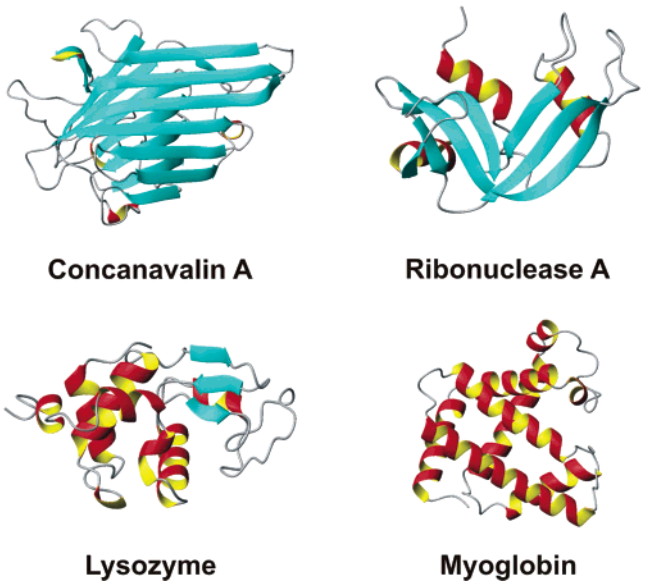

Figure 4. Ribbon diagrams of the four proteins investigated.

C. 2D IR Spectroscopy of β-Sheets in Proteins. To investigate the 2D IR spectroscopy of AP β-sheets in proteins of varying β-sheet content and size, we chose three globular proteins, concanavalin A (Con A), ribonuclease A (RNase A), and lysozyme (see Figure 4). These proteins contain 46%, 32%, and 6% AP β-sheet, and 0%, 18%, and 31% α-helix structure, respectively. Con A is the most extended system, with two relatively flat six-stranded AP β-sheets. RNase A has two domains that vary from two- to four-stranded regions. Lysozyme has a small three-stranded AP β-sheet region. We also studied myoglobin, with 74% α-helix content, as a system with no β-sheets. The 2D IR correlation spectra of these four proteins are given in Figure 5 together with their FTIR spectra.

The FTIR spectra show that, going from the exclusively AP β-sheet system Con A to exclusively α-helix system myoglobin, the peak amide I transition frequency blue-shifts from 1635 to 1650 cm^{-1} and the absorption lines in general become more symmetric. This trend is expected with increasing α-helix content. Nevertheless, it is difficult to correlate the spectral profiles observed in FTIR spectra with different structural elements present in this series of four proteins. In the FTIR spectra, the two-peak structure indicating the presence of an AP β-sheet is only evident in Con A, which shows a second, weak resonance at 1693 cm^{-1}. Although RNase A has 32% AP β-sheet content, only a weak shoulder is observed in the high-frequency edge of the amide I spectrum, while no such shoulder is present in lysozyme with 6.2% AP β-sheet.

The 2D IR spectra show considerably more structure and allow the β-sheet features not apparent in the FTIR spectra to be discerned. Con A shows the formation of cross-peaks between the strong and the weak amide I modes at $(\omega_1,\omega_3) = (1636,1698)$ and (1698,1636) cm^{-1}, indicating that the two

(38) Tokmakoff, A. *J. Phys. Chem. A* **2000**, *104*, 4247. Hybl, J. D.; Christophe, Y.; Jonas, D. M. *Chem. Phys.* **2001**, *266*, 295.

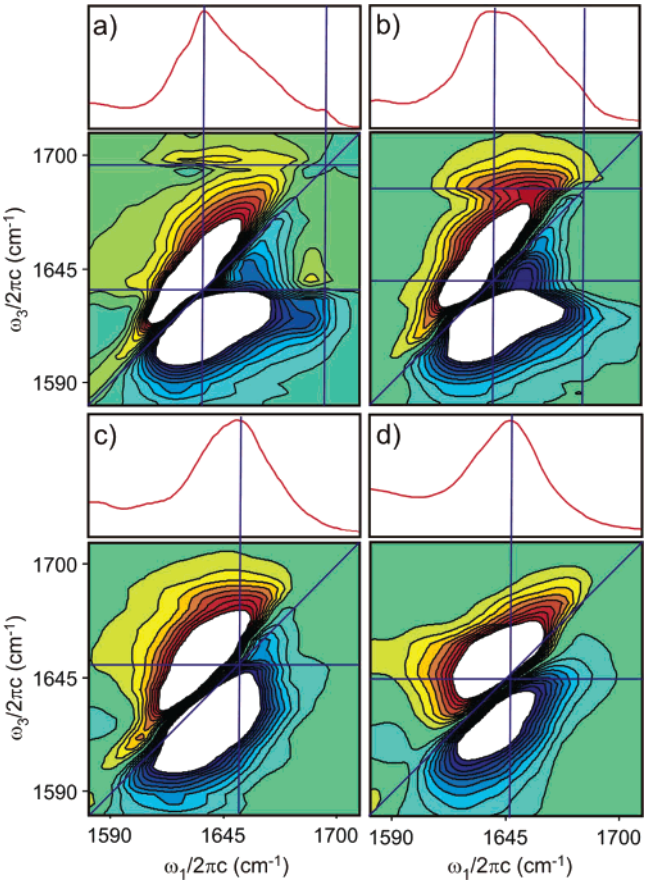

Figure 5. FTIR spectra and crossed-polarization 2D IR correlation spectra of the amide I transitions of (a) concanavalin A, (b) ribonuclease A, (c) lysozyme, and (d) myoglobin.

vibrations arise from the AP β-sheet structure. Anisotropy measurements of the cross-peak amplitude variation in parallel and crossed polarization configurations reveal that for Con A the apparent projection angle $\theta = 67° \pm 7°$. The projection angle determination, which in this case must account for the background intensity, involves separate analysis of the amplitudes in rephasing and nonrephasing spectra and is described further in the Supporting Information. Most of the spectral features observed in the FTIR spectrum contribute to the diagonally elongated features along the diagonal axis ($\omega_1 = \omega_3$). These are both the β-sheet diagonal peaks, as well as the disordered and turn regions, similar to the case of PLys. The cross-peak line shapes exhibit broadening characteristics similar to those of PLys, with the cross-peak at $(\omega_1,\omega_3) = (1636,1698)$ cm^{-1} elongating along ω_1. This is partially due to inhomogeneous broadening of the $\alpha-$ resonance, leading to constructive interference along ω_1 between a series of peaks at $\omega_3 = 1698$ cm^{-1}. Similarly, the cross-peak at $(\omega_1,\omega_3) = (1698,1636)$ cm^{-1} is strongly elongated along ω_1 at $\omega_3 = 1625$ cm^{-1} due to the same constructive interferences with the negative lobe of the $\alpha-$ diagonal peak. Additional cross-peaks may also arise between the $\alpha+$ resonance and the additional weak AP β-sheet resonances at $\sim$1660 cm^{-1}, such as those observed at $(\omega_1,\omega_3) = (1663,1640)$ cm^{-1} in Figure 2b, which could heighten the elongation effect. In the 2D IR amide I correlation spectrum of proteins, the overall effect of cross-peak formation and elongation along ω_1 for the features of the AP β-sheet, combined with additional resonances along the diagonal at 1650 cm^{-1}, leads to a "Z"-shaped pattern or contour profile.

With decreasing β-sheet size and content, the 2D IR cross-peaks are no longer clearly defined doublets, but rather elongate along ω_1 into ridges. The 2D IR spectrum for RNase A (Figure 5b) shows three features along the diagonal axis: the $\alpha-$ and $\alpha+$ resonances of the β-sheet, and a shoulder near 1650 cm^{-1}, presumably arising from the α-helices. The $\alpha-$ resonance peaks at $\sim$1636 cm^{-1} and appears inhomogeneously broadened. This leads to a strong positive cross-peak ridge for $\omega_3 = 1685$ cm^{-1} and parallel trough from negative going resonances at $\omega_3 = 1675$ cm^{-1}. The same constructive interference effects along ω_1 observed in Con A and PLys together with additional features on the diagonal lead to a "Z"-pattern in RNase A. Even though lysozyme (Figure 5c) is predominantly α-helix and the 2D spectrum is dominated by the diagonally elongated α-helix resonance(s) near 1650 cm^{-1}, a ridge or shoulder is observed for $\omega_3 = 1685$ cm^{-1}, indicating the presence of the AP β-sheet. This observation is further verified when compared to the same region of myoglobin (Figure 5d), an exclusively α-helix protein, which does not exhibit any ridge formation at all but has a diagonally elongated figure-8. Although the FTIR spectra for lysozyme and myoglobin are very similar in their shape and show no evidence of the $\alpha+$ and $\alpha-$ resonances, their 2D IR spectra are clearly different and reveal the underlying β-sheet content in lysozyme.

D. The Role of Conformational Disorder. Origin and Spectral Signatures of Disorder. The strong elongation of the diagonal $\alpha-$ peak in the β-sheet-containing proteins indicates an inhomogeneous frequency distribution. As opposed to the relatively large, ordered β-sheets in PLys, the β-sheet structures found in the proteins show considerable conformational variation, which in turn leads to variation of amide I transition frequencies. Elongation of the cross-peaks in the manner observed in the protein 2D IR spectra is also expected for inhomogeneous broadening in a system of coupled vibrations. For distributions, the cross-peak will stretch in a manner that reflects the statistical correlation of the frequency shifts between the $\alpha+$ and $\alpha-$ transitions.[11,16] The modeling of idealized β-sheets indicates that the $\alpha-$ transition frequency is sensitive to the number of strands and the magnitude of the interstrand couplings, whereas the $\alpha+$ frequency is not.[21] It is therefore expected that the cross-peak will elongate to reflect a broad distribution of $\alpha-$ frequencies and a narrow distribution of $\alpha+$ frequencies. The 2D IR spectrum can be interpreted as arising from a sum over many displaced resonances. Because resonances in 2D IR correlation spectra are oppositely signed doublets displaced along ω_3, this stretching effect is expected to be observed along ω_1 for the $\omega_1 < \omega_3$ cross-peak. For the second cross-peak for $\omega_1 > \omega_3$, destructive interferences between the oppositely signed contributions to a series of peaks along ω_3 will reduce or eliminate the effect.

There are a number of possible origins to the variation of $\alpha-$ frequencies observed in these spectra. Most likely, these arise from local configurational variation of the β-sheet within the native protein structure, but configurational disorder within the ensemble or dynamic effects such as structural or dielectric

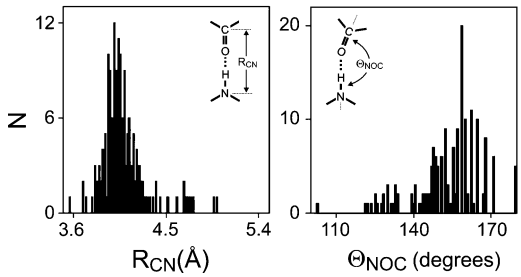

Figure 6. Histograms for the occurrence of interstrand distances along the CO···HN hydrogen bond, R_{CN}, and NOC interstrand angles along the CO···HN hydrogen bond, Θ_{NOC}, for the 136 hydrogen-bonded residues involved in the formation of AP β-sheets in the proteins studied in this work; taken from refs 42−45.

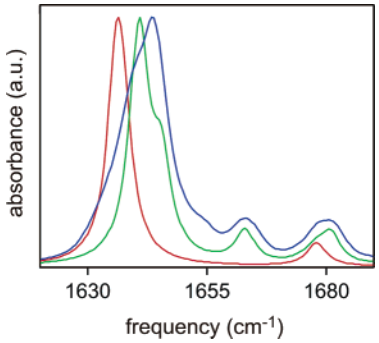

Figure 7. Calculated FTIR spectra of a planar AP β-sheet with six strands and 36 peptide groups. Normalized IR spectra are shown for calculations of (red) one ideal structure with periodic boundary conditions, (green) the same structure with open boundary conditions, and (blue) open boundary conditions averaged over random variation in position of amide I transition dipoles.

fluctuations can also affect the spectrum.[13,39] These effects ultimately lead to variation in the amide I transition frequencies at the individual amide sites (diagonal disorder) and variation in the coupling between them (off-diagonal disorder). Within these proteins, the β-sheet structure varies locally by the number of strands present, the interstrand geometry, and the curvature of strands. For example, RNase A is characterized by distorted β-sheets that vary between two and four hydrogen-bonded strands, depending on location. Variation in the number of strands influences the extent of delocalization of the vibrational excitation and the red-shift of the $\alpha-$ transition. Additionally, regions may vary by solvent exposure. Variations in the interstrand spacing, curvature, and solvent exposure all influence the strength and number of hydrogen bonds to the peptide groups making up the sheet, which act to shift the local amide I resonance frequency by tens of cm^{-1}.[40] The size of this effect suggests that static or dynamic variation in hydrogen-bonding conformation should be the dominant source of diagonal disorder, although the influence of conformation and through-bond effects on local electronic structure must also be considered.

Conformational variation within the β-sheets, whether static or dynamic, will also affect the strength of coupling between amide oscillators. Curvature in the strands or variation in the interstrand hydrogen-bonding distances and angle are expected even for a unique protein structure with β-sheets that deviate from planar.[41] These effects influence the orientation of amide I transition moments and separation of peptide units, both of which give rise to off-diagonal disorder. For the proteins studied here, we illustrate the considerable variation in interstrand spacing and orientation in Figure 6. Drawing on the AP β-sheet C═O···H−N hydrogen bonds observed in the crystal structures for the proteins studied here,[42−45] we plot a histogram of C···N distances (R_{CN}) and NOC angles (Θ). Interstrand spacing for these systems has a mean value of $\langle R_{CN}\rangle = 4.1$ Å with a standard deviation of 0.2 Å, while $\langle\Theta\rangle = 153°$ with a standard deviation of 13°. Presumably, these variations will have the largest effect on the short-range interstrand peptide interactions (L_{14}). Also for the somewhat weaker intrastrand interactions (L_{12}), the variation in *ab initio* calculated coupling strengths for the range of (ϕ,ψ) commonly associated with AP β-sheets can vary by 30%.[29,30,46]

To illustrate how small conformational disorder influences line-broadening in the amide I IR spectroscopy, we simulated the IR spectrum of an extended β-sheet under the influence of Gaussian disorder. (Direct calculations of 2D IR spectra of β-sheets with 30−100 oscillators and explicit structural disorder are prohibitively time-consuming at this point, and the numerical and analytical theory of these effects is the subject of ongoing work.) The IR spectrum of an idealized AP β-sheet of 36 peptide units arranged with six strands and six peptide units per strand was calculated using transition dipole coupling between amide I vibrations.[1] Off-diagonal disorder representative of small variations in interstrand spacing was introduced by randomly displacing the position of each amide I transition dipole in the x, y, and z directions, relative to its origin on the C═O bond 0.868 Å from the carbon. The displacements were chosen from a random Gaussian distribution with a standard deviation of 0.173 Å, equivalent to the variation in β-sheet interstrand distances observed in the crystal structure of Con A. The Hamiltonian for the one-quantum amide I states was diagonalized, yielding the energy eigenvalues, E_i. The transformation that diagonalizes the one-quantum Hamiltonian also transforms the transition dipole moments, μ_i, into the eigenbasis. The linear-IR spectrum is then calculated from $A(\omega) = -\mathrm{Im}\sum_i|\mu_i|^2/(\omega - E_i/\hbar + i\gamma)$, where the sum extends over the eigenstates and the damping γ is set to 4 cm^{-1}. Figure 7 shows the amide I spectrum calculated as an average of 140 000 disorder realizations.

For the IR spectroscopy of an ideal AP β-sheet, the $a-$ and $a+$ transitions appear at 1637 and 1678 cm^{-1} for the case of periodic boundary conditions. As seen in Figure 2b, in the finite system calculated with open boundary conditions, edge effects lead to an additional transition of mixed character in the 1660−1665 cm^{-1} region. Additionally, the $\alpha-$ transition is blue-shifted and shows a shoulder from additional resonances of somewhat different symmetry than the $a-$ state.

(39) Williams, R. B.; Loring, R. F.; Fayer, M. D. *J. Phys. Chem. B* **2001**, *105*, 4068. Merchant, K. A.; Noid, W. G.; Akiyama, R.; Finkelstein, I. J.; Goun, A.; McClain, B. L.; Loring, R. F.; Fayer, M. D. *J. Am. Chem. Soc.* **2003**, *125*, 13804.
(40) Torii, H.; Tasumi, M. *J. Raman Spectrosc.* **1998**, *29*, 537. Ham, S.; Kim, J.-H.; Lee, H.; Cho, M. *J. Chem. Phys.* **2003**, *118*, 3491. Kwac, K.; Cho, M. *J. Chem. Phys.* **2003**, *119*, 2247.
(41) Salemme, F. R. *Prog. Biophys. Mol. Biol.* **1983**, *42*, 95.
(42) Weisgerber, S.; Helliwell, J. R. *J. Chem. Soc., Faraday Trans.* **1993**, *89*, 2667.
(43) Oliveira, K. M.; Valente-Mesquita, V. L.; Botelho, M. M.; Sawyer, L.; Ferreira, S. T.; Polikarpov, I. *Trans. Eur. J. Biochem.* **2001**, *268*, 477.
(44) Chatani, E.; Hayashi, R.; Moriyama, H.; Ueki, T. *Protein Sci.* **2002**, *11*, 72.
(45) Rypniewski, W. R.; Holden, H. M.; Rayment, I. *Biochemistry* **1993**, *32*, 9851.
(46) Hamm, P.; Woutersen, S. *Bull. Chem. Soc. Jpn.* **2002**, *75*, 985.

For the case of disorder in the position of the transition dipole, the corresponding IR spectrum shows that the α+ transition is weakly affected by conformational variations, in terms of both central transition frequency and line width. On the other hand, the line shape of the α− transition is broadened as a result of its sensitivity to conformational variation and edge effects. This result indicates that configurational or energetic disorder will lead to a broad distribution of $\omega_{\alpha-}$, while the $\omega_{\alpha+}$ is narrow in comparison. This helps confirm the origin of the cross-peak line shape in the 2D IR spectra of PLys, Con A, and RNase A. A distribution of $\omega_{\alpha-}$ will lead to a $\omega_1 < \omega_3$ cross-peak that stretches out along $\omega_3 = \omega_{\alpha+}$. Symmetrically, the $\omega_1 > \omega_3$ cross-peak would stretch along ω_3, yet the destructive interferences between the positive and negative lobes of the cross-peak would act to suppress this effect in favor of the constructive interferences to the $\omega_{\alpha-}$ diagonal peak. Presently, we have only treated the example of off-diagonal disorder, but we expect that the addition of diagonal disorder to the energy of the amide I oscillators will further heighten the effects seen here. This is confirmed by Cho and co-workers, who have investigated the role of diagonal disorder on amide I spectra and delocalization in proteins.[3] Their results show a monotonic decrease in the amide I delocalization with increasing diagonal disorder, accompanied by a symmetric broadening of the features in the IR spectrum.

Sheet Size Dependence of Disorder and Delocalization. The excitonic vibrational states of the β-sheet structures will localize when the variance in the configurational and energetic disorder in the peptide sites exceeds the coupling strength between vibrations. For the case of AP β-sheets, the strength of interstrand couplings is considerably more than the interactions along the strands. This suggests that for β-sheets with modest local configurational variation within the sheet, such as changes in hydrogen-bonding geometry from the distortion of sheets, vibrational excitations should initially localize in the dimension along the strands. However, they may remain delocalized across multiple strands, in a direction either perpendicular or diagonal relative to the strands. When the nearest neighbor interstrand dimer pairs (such as 1−4 in Figure 1) remain strongly coupled, the delocalization direction will be dictated by the couplings between dimer pairs, which lie in diagonal directions in the plane of the sheet. For proteins such as RNase A in which the number of strands in a sheet varies within the protein, this would result in a number of IR-active states along the strands that vary in the extent of delocalization across multiple strands. This would be observed as a distribution of observed α− resonance frequencies. For high disorder comparable to the strongest interstrand coupling (L_{14}), the excitation would localize on the 1−4 dimers.

The 2D IR spectra give some insight into delocalization of the β-sheet vibrational excitations in the protein systems. For the extended β-sheet system Con A, the node of the cross-peak doublet along ω_3 lies at the fundamental frequency $\omega_{\alpha+}$, whereas in the case of the smaller three-stranded sheets of RNase A, the positive cross-peak ridge lies on resonance at $\omega_3 = \omega_{\alpha+}$. Additionally, the apparent line widths γ along ω_3 are narrower in the case of the Con A cross-peak. These observations highlight the much smaller cross-peak-doublet splitting ($\Delta_{\alpha+,\alpha-} < 4$ cm^{-1}) in the case of Con A. Because this splitting should roughly scale as the ratio of the amide I anharmonicity A to the delocalization number N, this observation indicates that the β-sheet excitations are far more delocalized in the case of Con A, given that the magnitudes of the amide I couplings are equivalent. In turn, N depends on the disorder.

The apparent increase in the degree of delocalization for the AP β-sheets of increasing size appears to reflect decreasing disorder for the larger sheets. Qualitatively speaking, larger extended AP β-sheets tend to be closer to planar, whereas significant twist is found in smaller ones.[34,41,47] Deviations from the idealized structure can be expected to lead to a decrease in the interstrand amide I couplings and variation in the interstrand hydrogen-bonding geometry, both of which act to localize the excitation. This helps to explain the monotonic decrease in the $\omega_{\alpha+,\alpha-}$ splitting observed in the 2D IR spectra with decreasing sheet size. An analysis of the intramolecular structural parameters of the AP β-sheet domains using the X-ray structures of Con A,[42] RNase A,[44] and lysozyme[45] reveals that the average value of the intramolecular hydrogen-bonding angle between the strands decreases as the percentage of AP β-sheet decreases: from 157° in Con A, to 148° in RNase A, and to 138° in lysozyme. Smaller hydrogen-bonding angles imply weaker hydrogen bonds and higher amide I frequencies, which is evident in the blue-shifts of the stronger amide I transition going from Con A to lysozyme.

A quantitative determination of the degree of delocalization across the strands will require more detailed models of short-range amide I couplings that account for variation in hydrogen-bonding geometry, but qualitative comparisons with our idealized model would suggest that in Con A this would be at least three or four strands. This can be compared with calculations of the extent of delocalization of β-sheet excitations in Flavidoxin, which suggest that such excitations can be delocalized over tens of oscillators and other secondary structures.[3] Also, in 2D IR studies of small proteins, delocalization lengths on the order of 8 Å were determined,[17] and the delocalization length determined for amide I vibrations in an α-helical peptide was found to be approximately one turn or four peptide units of the helix.[18] The β-sheet delocalization length should also be reflected in the projection angle between the α− and α+ transitions, θ. In the case of Con A, the value of $\theta = 67° \pm 7°$ spans the range of projection angles between $\boldsymbol{\mu}_{a+}$ and $\boldsymbol{\mu}_{a-}$ that our calculations associate with four or more strands.

Concluding Remarks

Two-dimensional IR spectroscopy of the amide I transitions of PLys and β-sheet-containing proteins indicates that this method can be used to gain considerable insight into β-sheet structure and structural variation for proteins in solution. This information is viewed through the delocalized amide I vibrational excitations associated with the secondary structure. Analysis of the peak positions, amplitudes, and line shapes allows insight into the size of the sheets, the orientation of the transition moments, and the degree of structural disorder in the sheet. The two dominant IR-active transitions of an AP β-sheet, α+ and α−, can be observed in 2D IR spectra as cross-peaks, even when not apparent in the traditional FTIR spectrum. Interference effects between the resonances that form the diagonal and cross-peaks together with additional features along

(47) Stanger, H. E.; Syud, F. A.; Espinoza, J. F.; Giriat, I.; Muir, T.; Gellman, S. H. *Proc. Natl. Acad. Sci. U.S.A.* **2001**, *98*, 12015.

the diagonal lead to a characteristic "Z"-shaped signature for AP β-sheet secondary structure. Favorable comparisons to the predictions of a simple model for the amide I vibrational spectroscopy of AP β-sheets indicate that the interstrand interactions are considerably stronger than the intrastrand interactions. This suggests that it is possible to relate the position of cross-peaks to the number of strands in the sheet. The position of the peak is related to the $\alpha+/\alpha-$ transition splitting $\omega_{\alpha+,\alpha-}$, which is strongly influenced by interstrand couplings. Beyond describing vibrational couplings, the cross-peak line shape is related to the energetic and conformational disorder of the sheet, such as variations in hydrogen bonding or other conformational variations within the sheet and from one sheet to another. Additionally, the amplitude of the cross-peak can be related to the orientation of the $\alpha+$ and $\alpha-$ transition moments, and the frequency splitting of the cross-peak is a measure of the delocalization length of the amide vibrations of the sheet.

These observations are based on trends for the few proteins studied here. A more complete picture of the relationship between spectral features and β-sheet structure, including the underlying vibrational couplings, should be further scrutinized with a wide-ranging sample of proteins and model peptides, in addition to temperature- and solvent-dependent studies. The ability to pursue such studies is now becoming possible with the rapid development of 2D IR spectroscopy. Nonetheless, the examples presented here indicate that 2D IR spectra on amide I bands offer a sensitive measure of β-sheet content and more detailed structural variables. Quantitative modeling of these spectra relies on further development of general models for vibrational couplings in proteins. This is particularly the case for short-range interactions (where the transition dipole coupling model has limited success), through-bond interactions, and the influences of hydrogen bonding. Additionally, simplified analytical models and numerical methods of introducing the effects of structural and energetic disorder in such calculations are needed. Even with the considerable complexity involved, the development of general models for protein vibrational spectroscopy is now an area of renewed interest and rapid advances.[3,10,21,48]

2D IR spectroscopy and other nonlinear-IR techniques should provide both meaningful tests of such models and, ultimately, detailed investigative tools for protein research. While the structural information obtained in IR spectroscopy is not atomistic in nature, it does probe delocalized or collective coordinates that can be sensitive to mesoscopic structure and conformation. Additionally, as a fast time-scale probe, vibrational spectroscopy reveals structural information transiently with a picosecond window. These characteristics are those optimal for studies of fast kinetics and dynamics of protein conformational changes.

Acknowledgment. We thank Peter Hamm, Hajime Torii, and Minhaeng Cho for sharing their calculations of intrastrand amide I couplings from refs 46, 29, and 30, respectively. We thank Joel Eaves for his advice on the Gaussian disorder calculation, Matt DeCamp for experimental assistance, and Arend Dijkstra for conversations on the nature of amide I eigenstates for β-sheets. This work was supported by the National Science Foundation (Grant CHE-0316736), the National Parkinson Foundation, and the Petroleum Research Fund of the American Chemical Society. A.T. thanks the Alfred P. Sloan Foundation and the David and Lucile Packard Foundation for their fellowship support.

Supporting Information Available: Details of the data analysis for determining the $\boldsymbol{\mu}_{\alpha+}/\boldsymbol{\mu}_{\alpha-}$ projection angle in concanavalin A. This material is available free of charge via the Internet at http://pubs.acs.org.

JA049811J

(48) Gerber, R. B.; Brauer, B.; Gregurick, S. K.; Chaban, G. M. *PhysChemComm* **2002**, 142. Gerber, R. B. C., G. M.; Gregurick, S. K.; Brauer, B. *Biopolymers* **2003**, *69*, 370. Choi, J.-H.; Ham, S.; Cho, M. *J. Phys. Chem. B* **2003**, *107*, 9132.